5-27-1954

Cosmic Ray Intensity at Balloon Altitudes

Kenneth R. Greider

COSMIC RAY INTENSITY AT BALLOON ALTITUDES

By

Kenneth R. Greider

A Thesis

In partial fulfillment of the

Requirements for the Degree of

Master of Science in Physics

The University of New Mexico

1954

This thesis, directed and approved by the candidate's committee, has been accepted by the Graduate Committee of the University of New Mexico in partial fulfillment of the requirements for the degree of

MASTER OF SCIENCE

E. H. Castetter
DEAN

5/27/54
DATE

Thesis committee

Robert R. Brown
CHAIRMAN

John R. Green

Victor H. Reynier

TABLE OF CONTENTS

CHAPTER		PAGE
I.	INTRODUCTION	1
	A. History and Summary of the Problem	1
	B. Definitions	3
	C. Experimental Techniques	4
II.	THEORY	6
	A. Motion of Charged Particles in the Earth's magnetic Field	6
	B. The Low Energy Cut-Off	8
	C. Periodic Intensity Variations	14
	D. Non-periodic Intensity Variations	15
III.	EXPERIMENTAL PROCEDURE	18
	A. Equipment	18
	B. Operation	20
IV.	RESULTS	25
	A. History of Flights	25
	B. Interpretation of Data	27
V.	CONCLUSIONS	32
BIBLIOGRAPHY		35

LIST OF FIGURES

FIGURE		PAGE
1.	Plot of trajectory in the equatorial plane	9
2.	Variation of primary cosmic ray flux with latitude above the atmosphere	13
3.	Schematic diagram of the oscillator power supply	19
4.	Schematic diagram of multivibrator and F.M. transmitter	21
5.	Photograph of gondola and case	22
6.	Schematic diagram of saturation amplifier and integrating circuit	23
7.	Counting rate for flight 6	28
8.	Counting rate for flight 3	29
9.	Counting rate for flight 2	30

LIST OF TABLES

TABLE		PAGE
I.	Momentum and Energy values for Allowed Cones for $\lambda=0^{\circ}$ and $\lambda=45^{\circ}$N.	12
II.	Summary of flights launched during April, 1954	26

CHAPTER I

INTRODUCTION

A. History and Summary of the Problem

In the investigation of cosmic rays at balloon altitudes, it is important to recognize the various factors that affect the total intensity at any point in the atmosphere. The three main factors are

1. Atmospheric influences: variations of intensity with atmospheric depth[1],
2. Geomagnetic influences: variations of intensity with the geomagnetic latitude, and
3. Extraterrestial influences: periodic and non-periodic variations of intensity.

If the distribution of primary cosmic rays, consisting mostly of protons and alpha particles, is isotropic in outer space, then a counting apparatus located beyond the earth's atmosphere will record a constant flux of particles. However, as these energetic particles penetrate the atmosphere, they collide with nuclei of the air and produce secondary particles. In energetic collisions of this sort, not only heavy particles such a protons, neutrons, and alpha particles, but also light particles such as pi and mu mesons and electrons are given off. With the production of secondary particles, the number and average

---

[1] A list of definitions is given in the following section.

energy of the primary particles decrease with atmospheric depth while the total number of particles increases. A maximum flux is reached at an atmospheric depth where the absorption rate of secondaries by ionization processes equals the production rate. The height of the maximum flux in the atmosphere will depend on the local meteorological conditions of temperature and pressure as well as the energy distribution of the incident radiation. Beyond this maximum, absorption processes begin to dominate, and the flux decreases.

The earth has a magnetic field and thereby acts as a magnetic spectrometer by deflecting the charged particles of the primary cosmic ray beam. Near the geomagnetic equator, where the lines of magnetic intensity are perpendicular to vertically incident particles, a large force acts on the particles and permits only the most energetic to strike the earth. Since the lines of magnetic intensity make smaller angles with vertically incident particles as the geomagnetic latitude increases, the cut-off energy decreases and particles of lower energy reach the earth. At the geomagnetic pole particles of all energies can strike the earth. The total cosmic ray intensity at any given atmospheric depth, therefore, is dependent on the geomagnetic latitude. Van Allen[1] has recently investigated this phenomenon, known as the latitude effect, at altitudes up to 300 miles. He has found that beyond the atmosphere the ratio of polar intensity to equatorial intensity is

about 10.

Extraterrestial influences, such as a possible general solar magnetic field, will affect the cosmic radiation received at the earth. Such a field would cut off the low end of the energy spectrum of primary particles in the vicinity of the earth in the same manner as the earth's field cuts off the energy spectrum at a given geomagnetic latitude. This problem has been treated theoretically by Kane, Shanley, and Wheeler[2], and Dwight[3], and experiments have been performed to ascertain whether a solar field exists. Due to the various periodicities of relative orientation in the earth-sun system, various types of periodic variations in primary cosmic ray intensity on the earth would occur.

Non-periodic extraterrestial influences such as magnetic storms on the earth and solar flares have also been found to cause variations in cosmic ray intensity. Because of the nature of these effects, they cannot be predicted in advance. Since only a limited amount of data is available, the actual mechanisms involved are not clearly understood at the present time.

B. Definitions

The following is a list of definitions of terms used in this thesis:

Atmospheric Depth: The mass of air per unit area ($gm\ cm^{-2}$) above any given level in the atmosphere.

Flux: The number of particles incident on a unit area per unit time per unit solid angle (cm^{-2} sec^{-1} $steradian^{-1}$).

Cut-Off Energy: The energy of a particle whose trajectory is such that it just grazes the earth.

Impact parameter: The perpendicular distance from a point to the extension of the original line of motion of a particle.

C. Experimental Techniques

Experimental investigations of cosmic ray intensities have been made by using particle detectors such as ionization chambers, Geiger counters, and nuclear emulsions. Detectors such as ionization chambers, single Geiger counters, and nuclear emulsions are sensitive to particles coming from all directions, whereas with the application of coincidence techniques, directional intensities can be obtained.

In the experiment described in Chapter IV, individual Geiger counters were carried by balloons to high altitudes to observe the total cosmic ray intensity. Several flights were made over a period of a few weeks to see what variations, if any, occurred in the maximum intensity. Since variations in the maximum intensity at a given geomagnetic latitude are caused only by extraterrestial factors, such variations, if observed, might help explain some of the periodic or non-periodic influences on the energy spectrum of primary cosmic rays. In order that the recovery of the equipment should not be a problem, the information from the Geiger

counter was transmitted by radio to a recording station on the ground.

CHAPTER II

THEORY

A. Motion of Charged Particles in the Earth's Magnetic Field

Detailed analyses of the motion of charged particles in the geomagnetic field have been carried out by Störmer, Vallarta, Lemaitre, and others, and have been reviewed by Fermi.[4]

In order to describe accurately the motion of particles in a magnetic field, it is best to use the Lagrangian formalism. The Lagrangian for a particle having a mass m, and a charge Ze, and moving with a velocity $\vec{v}$ in a magnetic field of vector potential $\vec{A}$, is

$$\mathcal{L} = -mc^2\sqrt{1-\beta^2} + \frac{Ze}{c}\vec{A}\cdot\vec{v}, \qquad (1)$$

where c is the velocity of light and β is the ratio v/c. In spherical polar co-ordinates in which λ is the latitude angle, ϕ the azimuth angle increasing toward the west, and r the radius, the vector potential becomes

$$\vec{A} = \mu\frac{\cos\lambda}{r^2}\vec{e}_\phi, \qquad (2)$$

where $\vec{e}_\phi$ is the unit vector at (r,λ,ϕ) pointing in the direction of increasing ϕ, and μ is the magnitude of the earth's dipole moment. Lagrange's equations then consist of a set of three partial differential equations,

$$\frac{\partial \mathcal{L}}{\partial r} = \frac{d}{dt}\left(\frac{\partial \mathcal{L}}{\partial \dot{r}}\right)$$

$$\frac{\partial \mathcal{L}}{\partial \lambda} = \frac{d}{dt}\left(\frac{\partial \mathcal{L}}{\partial \dot{\lambda}}\right) \qquad (3)$$

$$\frac{\partial \mathcal{L}}{\partial \phi} = \frac{d}{dt}\left(\frac{\partial \mathcal{L}}{\partial \dot{\phi}}\right).$$

While in general it is not possible to obtain solutions for these equations in closed form, it is possible to solve them by numerical integration; in this manner the trajectory of a particle approaching the earth can be described accurately.

To develop the theory further, consider Lagrange's equation in ϕ and $\dot{\phi}$. It is seen that

$$\frac{\partial \mathcal{L}}{\partial \phi} = \frac{d}{dt}\left(\frac{\partial \mathcal{L}}{\partial \dot{\phi}}\right) = 0 \qquad (4)$$

since $\mathcal{L}$ is independent of ϕ. Thus the generalized component of angular momentum

$$p_\phi = \frac{\partial \mathcal{L}}{\partial \dot{\phi}} = -mc^2 \frac{\partial}{\partial v}\left[(1-\beta^2)^{1/2}\right]\frac{\partial v}{\partial \phi} + \frac{Zc\mu}{rc}\cos^2\lambda \qquad (5)$$

is constant and is an integral of the motion. Since

$$\beta = \frac{v}{c} = \frac{\sqrt{\dot{r}^2 + r^2\dot{\lambda}^2 + r^2\cos^2\lambda\,\dot{\phi}^2}}{c},$$

it follows that

$$p_\phi = \frac{mvr^2\cos^2\lambda}{\sqrt{1-\beta^2}\,v}\dot{\phi} + \frac{Ze}{rc}\mu\cos^2\lambda, \qquad (6)$$

and the ratio

$$\frac{p_\phi}{p} = r^2\cos^2\lambda\frac{\dot{\phi}}{v} + \frac{\mu}{p}\frac{\cos^2\lambda}{r} = b, \qquad (7)$$

.ion

where b is the impact parameter and P is the magnetic rigidity, pc/Ze.

As an illustration of the solution of this equation, consider the case of motion confined to the equatorial plane for which $\lambda = 0$ and $\dot{\lambda} = 0$. Equation (7) then becomes

$$b = r^2 \frac{\dot{\phi}}{v} + \frac{\mu}{Pr} \quad . \tag{8}$$

From this equation ϕ can be obtained in terms of r,

$$\phi = \int \frac{\left(b - \frac{\mu}{Pr}\right)}{r^2 \left[1 - \left(\frac{b}{r} - \frac{\mu}{Pr^2}\right)^2\right]^{1/2}} dr . \tag{9}$$

Since only the co-ordinates r and ϕ are needed to describe motion in the equatorial plane, a typical trajectory in that plane results from the integration of equation (9). In Figure 1 is shown such a trajectory for which Z=1, p=10.3 BeV/c, $\mu = 8.1 \times 10^{25}$ gauss-cm^3, and $b = 4.83\ r_e$, where r_e is the earth's radius. The importance of these trajectories will become apparent in section C, which deals with periodic intensity variations.

B. The Low Energy Cut-Off

Consider again equation (7) which is an integral of the motion since both p_ϕ and p are constant. Since

$$v_\phi = r \cos\lambda \, \dot{\phi},$$

then

$$b = r \cos\lambda \frac{v_\phi}{v} + \frac{\mu}{P} \frac{\cos^2\lambda}{r} \quad ,$$

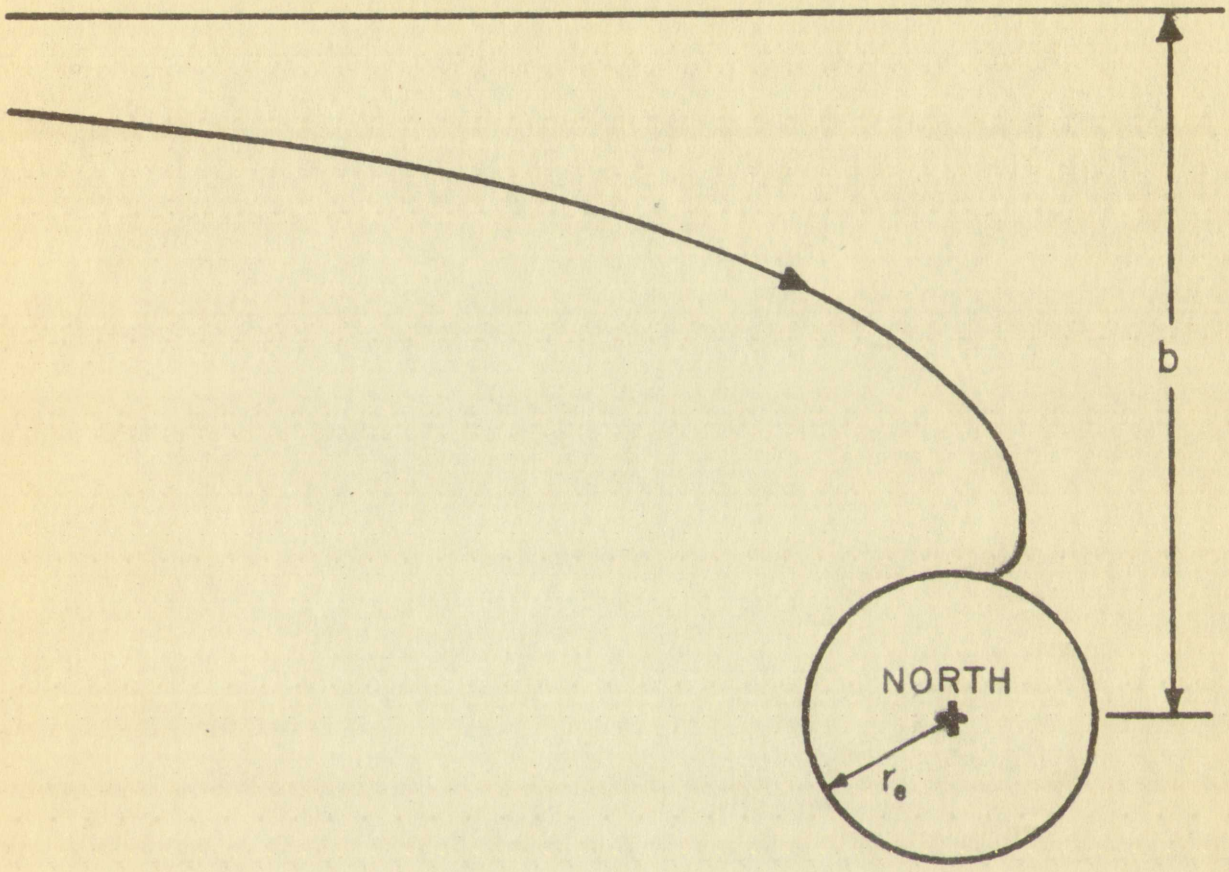

Figure 1. Plot of the trajectory in the equatorial plane for Z=1, p=10.3 BeV/c, and b=4.83 r_e.

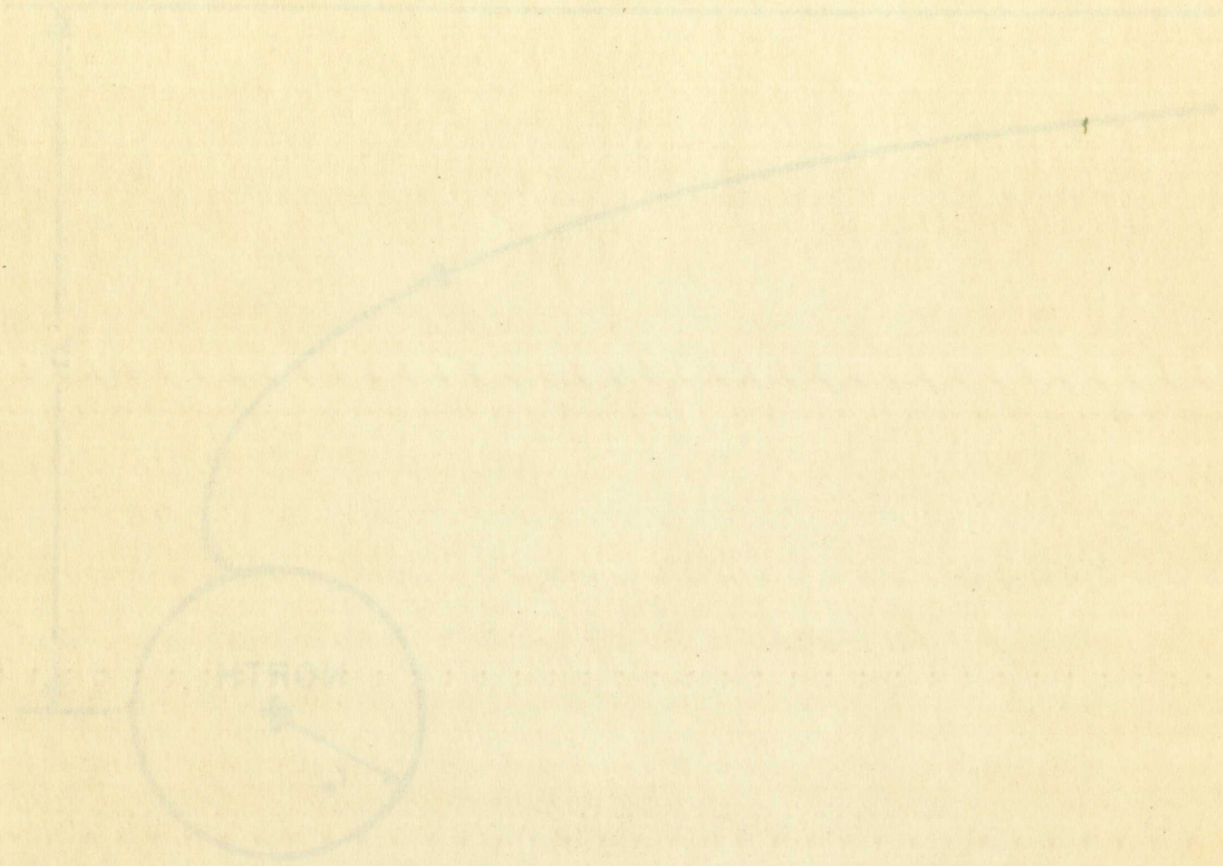

and the Störmer relation

$$b = r\cos\lambda\cos\gamma + \frac{\mu}{p}\frac{\cos^2\lambda}{r} \tag{10}$$

is obtained. γ is the angle between v and v_ϕ. If all distances are expressed in terms of the length $\sqrt{\frac{\mu}{p}}$, so that $r=R\sqrt{\frac{\mu}{p}}$ and $b=B\sqrt{\frac{\mu}{p}}$, equation (10) becomes dimensionless,

$$B = R\cos\lambda\cos\gamma + \frac{\cos^2\lambda}{R} . \tag{11}$$

Then it follows that

$$\cos\gamma = \frac{B}{R\cos\lambda} - \frac{\cos\lambda}{R^2} . \tag{12}$$

While certain values of B, R, and λ for which $|\cos\gamma| \leq 1$, define allowed regions for the particle, other values of B, R, and λ for which $|\cos\gamma| > 1$ define forbidden regions for the particle. In particular, if the energy of a particle coming from infinity is less than 60Z BeV, then R at the earth is less than 1, and in order for the particle to reach the earth, B must be less than 2. If this restriction on B is substituted into equation (12), it follows that

$$\cos\gamma < \frac{2}{R\cos\lambda} - \frac{\cos\lambda}{R^2} . \tag{13}$$

From equation (13) it is seen that particles at a given latitude and with a given momentum can reach the earth only from a cone whose half angle is $180^\circ-\gamma$. As the momentum decreases, the angle of the cone decreases until the critical value of momentum is reached for which $\gamma=180^\circ$. This critical momentum is called the cut-off momentum since particles of lower momenta than this will never strike the

earth at that latitude. The corresponding cut-off energy can be computed from relativistic theory. Values for the minimum cones are given in Table I for $\lambda=0^\circ$ and $\lambda=45^\circ$, the latter being the geomagnetic latitude of Albuquerque.

In order that the dependence of cosmic ray intensity on latitude be found, equation (13) must first be solved for the cut-off momentum. This is done by substituting $R=r\sqrt{\frac{Ze\mu}{pc}}$, allowing $\gamma=$ to equal 180°, and solving for the momentum, p,

$$p = 60Z\left[\frac{1-\sqrt{1+\cos^3\lambda}}{-\cos\lambda}\right]^2. \qquad (14)$$

The numerical constants have been evaluated so that the units of p are BeV/c. Second, a differential momentum spectrum for primary cosmic radiation must be assumed. From experimental data such a spectrum might be represented by an expression:

$$dN \sim p^{-4.4}dp\,, \qquad (15)$$

where dN is the number of primary protons whose momenta lie between p and p+dp. If both equations (14) and (15) are considered, it is seen that the latitude effect causes the intensity of primary cosmic radiation to increase with increasing geomagnetic latitude. Verification of this is shown by the experimental results of Van Allen which are reproduced in Figure 2.

TABLE I

MOMENTUM AND ENERGY VALUES FOR ALLOWED CONES FOR $\lambda=0^\circ$ AND $\lambda=45^\circ$N (ALBUQUERQUE)

Minimum Cone Half Angle (degrees)	Energy $\lambda=0^\circ$ (BeV)	Momentum $\lambda=0^\circ$ (BeV/c)	Energy $\lambda=45^\circ$ (BeV)	Momentum $\lambda=45^\circ$ (BeV/c)
180	9.4	10.3	3.83	4.68
150	9.7	10.6	3.66	4.50
120	10.9	11.8	3.38	4.22
90	14.1	15.0	2.92	3.75
60	19.6	20.5	2.41	3.22
30	31.3	32.2	2.36	3.17
0	59.1	60.0	2.31	3.10

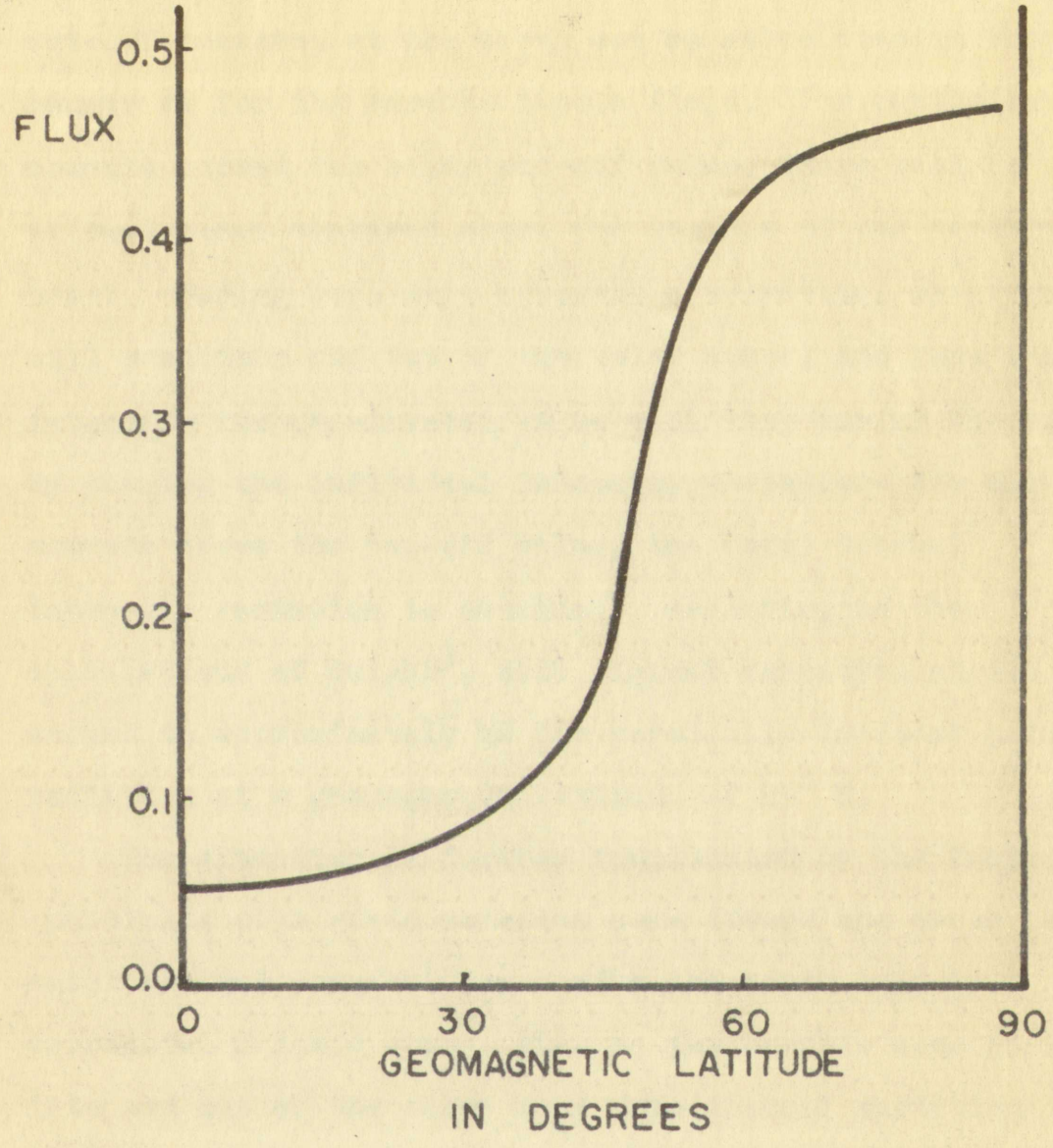

Figure 2. Variation of primary cosmic ray flux with latitude above the atmosphere.

variation, but also the phase, which gives a time scale to the variation.

In addition to the diurnal periodicity mentioned above, intensity variations may be caused by the sun's rotational period of about 26 days. If there should be an angle between the sun's axis and the presumed solar dipole moment, such variation in intensity would result at any point in space because of the continual change in heliomagnetic latitude. For a given particle momentum, this latitude variation changes the size of the allowed cone, and the integrated effect for all momenta changes the total intensity. Even if the sun's axis and dipole moment should be parallel, the fact that the ecliptic is inclined 7° from the solar equatorial plane would result in a yearly intensity variation. In all of these cases the periodic variations in intensity would be observed in experiments performed above the atmosphere.

D. Non-periodic Intensity Variations

There are two other types of intensity variations, both of which are believed to be due to solar disturbances: terrestial magnetic storms and solar flares. The former, which decrease the horizontal component of the earth's magnetic intensity, are often correlated with decreases of as much as 5% in cosmic ray intensity. Such intensity variations, however, are short lived, and the intensity returns to normal after a few days.

According to Chapman[5] the sun releases positive ions and electrons as a result of solar disturbance. When these particles arrive near the earth, their trajectories are deflected in opposite directions according to the charge on the particle, and the particles travel around the earth in curved paths much like the primary protons discussed in section A, above. These moving charges constitute an electric current, called a ring current. This current induces a magnetic field which opposes the earth's field between the ring current and the earth, and which reinforces the earth's field outside the ring. During a magnetic storm, therefore, the terrestial horizontal component of the magnetic intensity decreases, and the cosmic ray intensity also decreases since the stronger field outside the ring deflects away from the earth certain low-energy charged primaries that normally would have been observed. If the time for the solar disturbance is long compared with the 26 day solar period, a 26 day recurrence variation will result since the disturbance periodically rotates into the line of sight of the earth. Various analyses suggest such a 26-day cosmic-ray intensity variation of about 0.4%.

Major solar disturbances produce large sunspots and solar flares which are accompanied by sudden increases in the cosmic ray intensity at the earth. Since 1937 only 4 such flares have been observed.[6] Usually the intensity increases approximately 10% about one hour after the flare is first observed on the sun, and in a day drops to a sub-

normal value as in a magnetic storm. Final recovery to normal intensity occurs over several days. Several explanations of the intensity increases have been proposed, but due to the lack of data, there is no interpretation generally accepted as correct. Observations of the non-periodic cosmic ray variations can be made above the atmosphere by measuring the cosmic-ray intensity at regular time intervals or by immediately recording the intensity variation after an observed solar disturbance.

CHAPTER III

EXPERIMENTAL PROCEDURE

A. Equipment

The Geiger counters used in this experiment were made of 1 inch O.D. brass tubing having a wall thickness of 1/64-inch. The central wire of the counter consisted of a 0.005-inch diameter Kovar wire whose effective length was 9 inches. The counters were filled with a 10:1 argon-ether mixture to a pressure of about 11 cm. Hg.; with this gas filling the Geiger threshold was approximately 1150 volts. The operating point of each counter was then maintained at 1200 volts by a regulated oscillator power supply whose circuit is shown in Figure 3. By allowing the counters to register approximately 10,000 counts prior to each flight, a counting rate on the ground was obtained.

Pulses from the Geiger counter were shaped into square waves of 1.45-millisecond duration by a multivibrator and were then applied to the reactance modulator of a frequency modulated transmitter operating on a frequency of 103 megacycles per second. By changing the reactance of the plate circuit of the oscillator, the square waves deviated the transmitting frequency by approximately 75 kilocycles per sec. The 0.1 watt of r.f. power developed by the oscillator was then radiated by a half-wave, center-fed coaxial antenna. The complete circuit of the

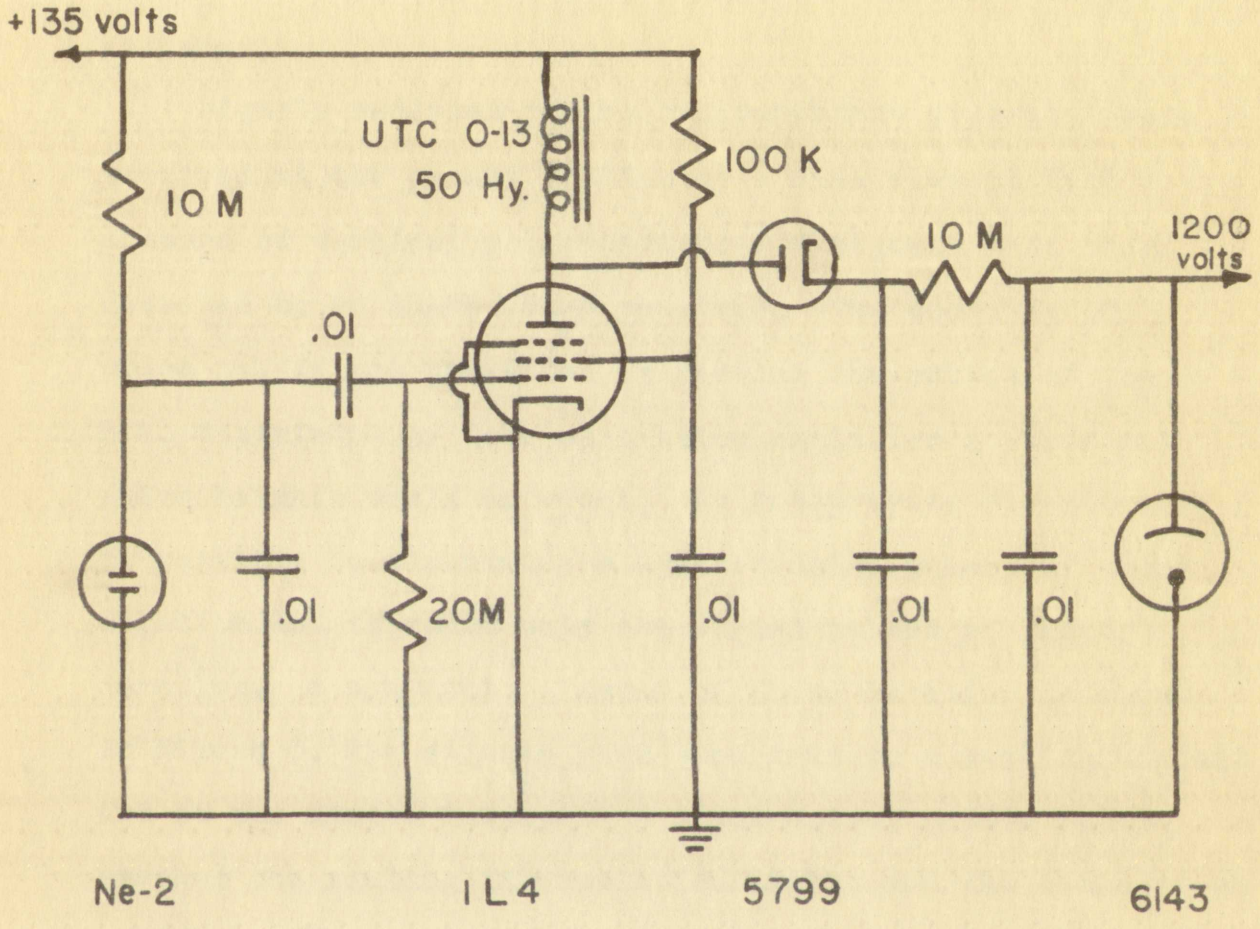

Figure 3. Schematic diagram of the oscillator power supply.

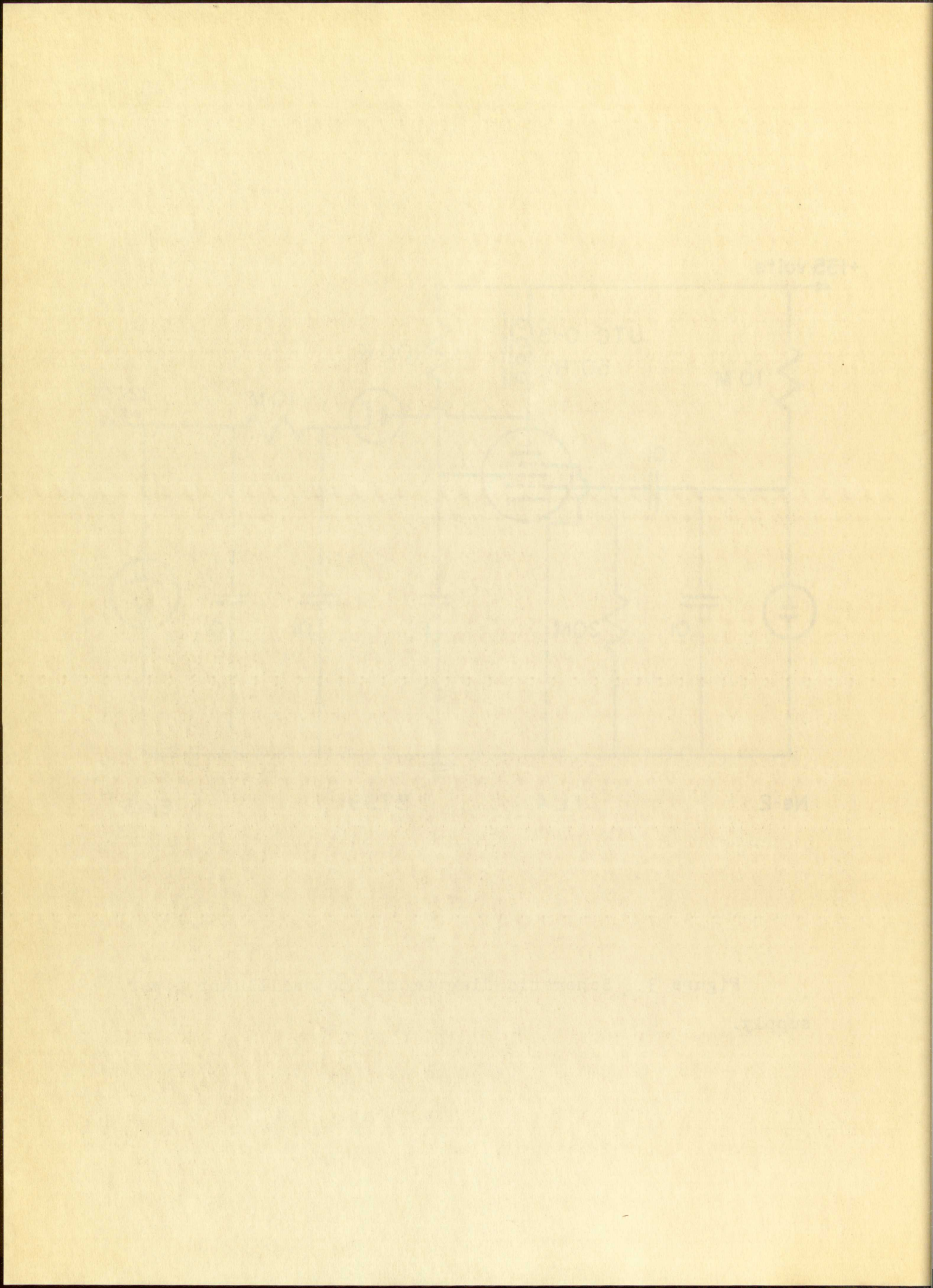

F.M. oscillator and related components is shown in Figure 4. Figure 5 shows the entire apparatus which measured approximately 6"x6"x18" and weighed 3 kg. A Styrofoam case served both as a thermal insulator and as a shock absorber.

Signals radiated by the balloon-borne apparatus were received at the ground station by a five element Yagi antenna of vertical polarization. The signals were then detected by an AM-FM ARR-5 receiver. The counting of noise pulses was prevented by feeding the output of the F.M. discriminator to a saturation amplifier so that all pulse heights would be equal. An integrating circuit made it possible to discriminate against noise pulses of short duration and to count only the signal pulses of longer duration. A schematic diagram of these circuits is shown in Figure 6. The signals were then sent to a scaling circuit and at one minute intervals a clock-driven camera photographed the scaling interpolation lights and the scale-of-64 register. The pictures were visually examined to obtain the counting rate of the counter.

B. Operation

Two Dewey-Almy J8-18-800 balloons were used to carry the equipment aloft. The free lift of the balloons was adjusted for an ascension rate of 1000 feet per minute. The balloons rose to approximately 90,000 feet, where the bursting of one balloon allowed the apparatus to descend.

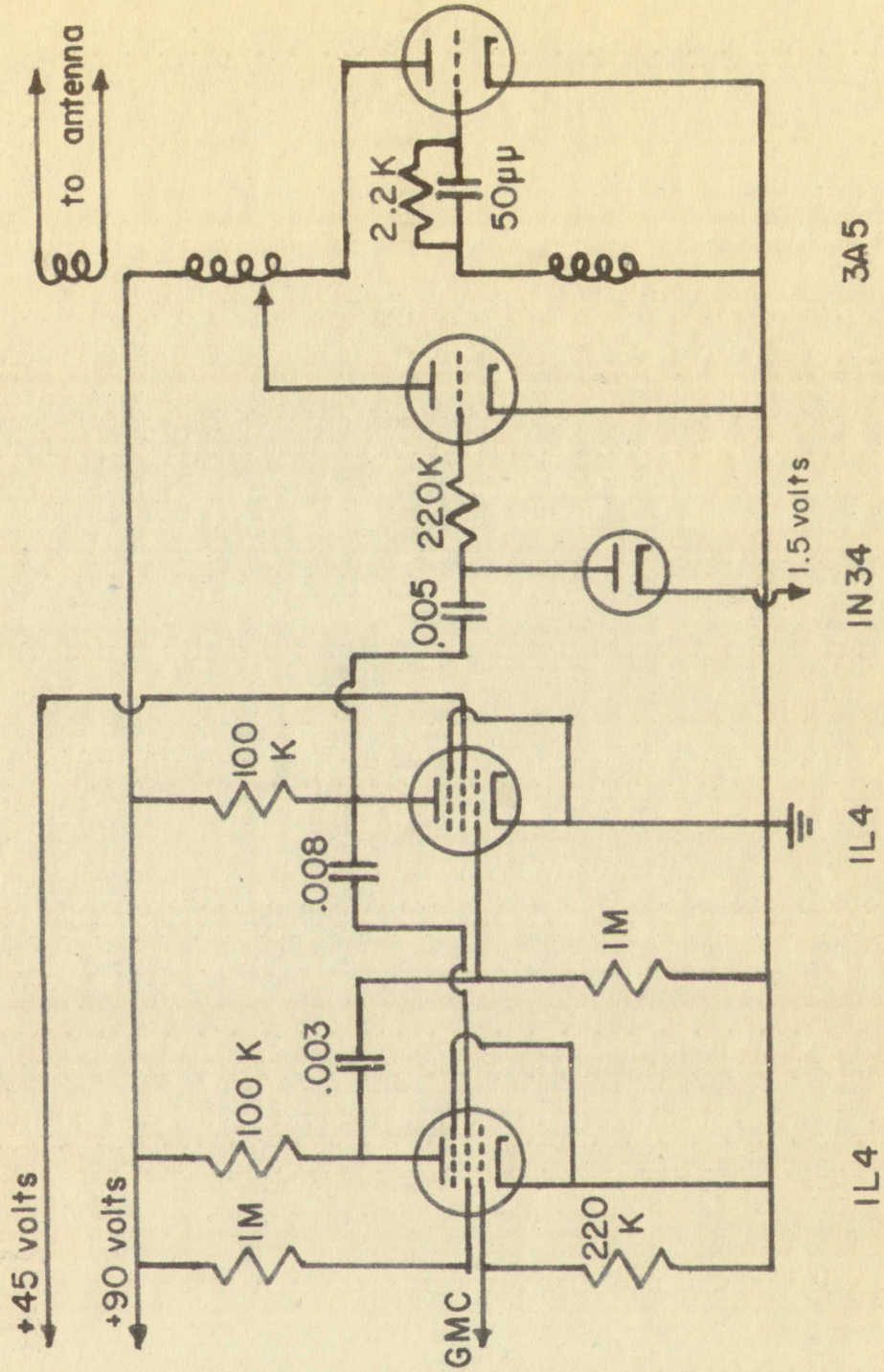

Figure 4. Schematic diagram of multivibrator, reactance modulator, and F.M. oscillator.

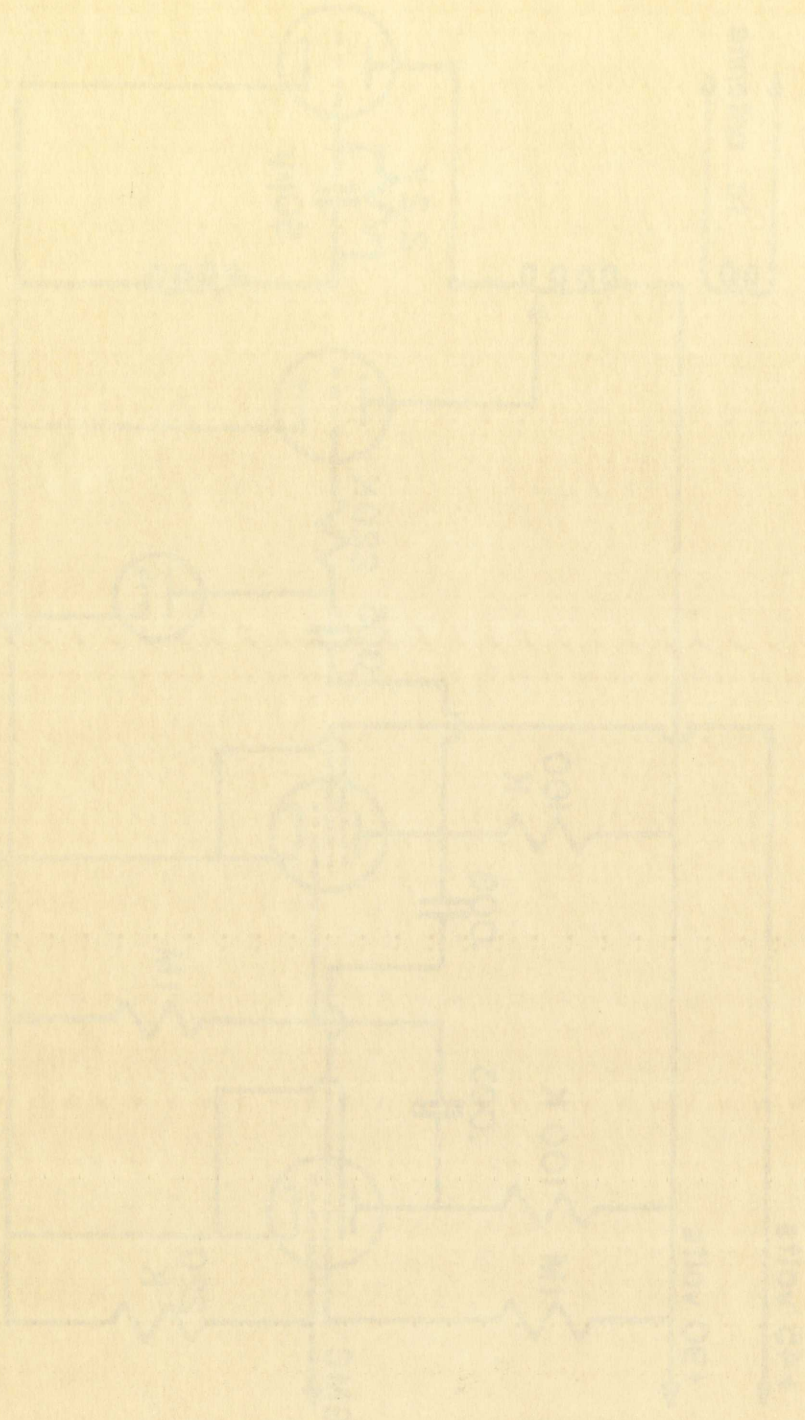

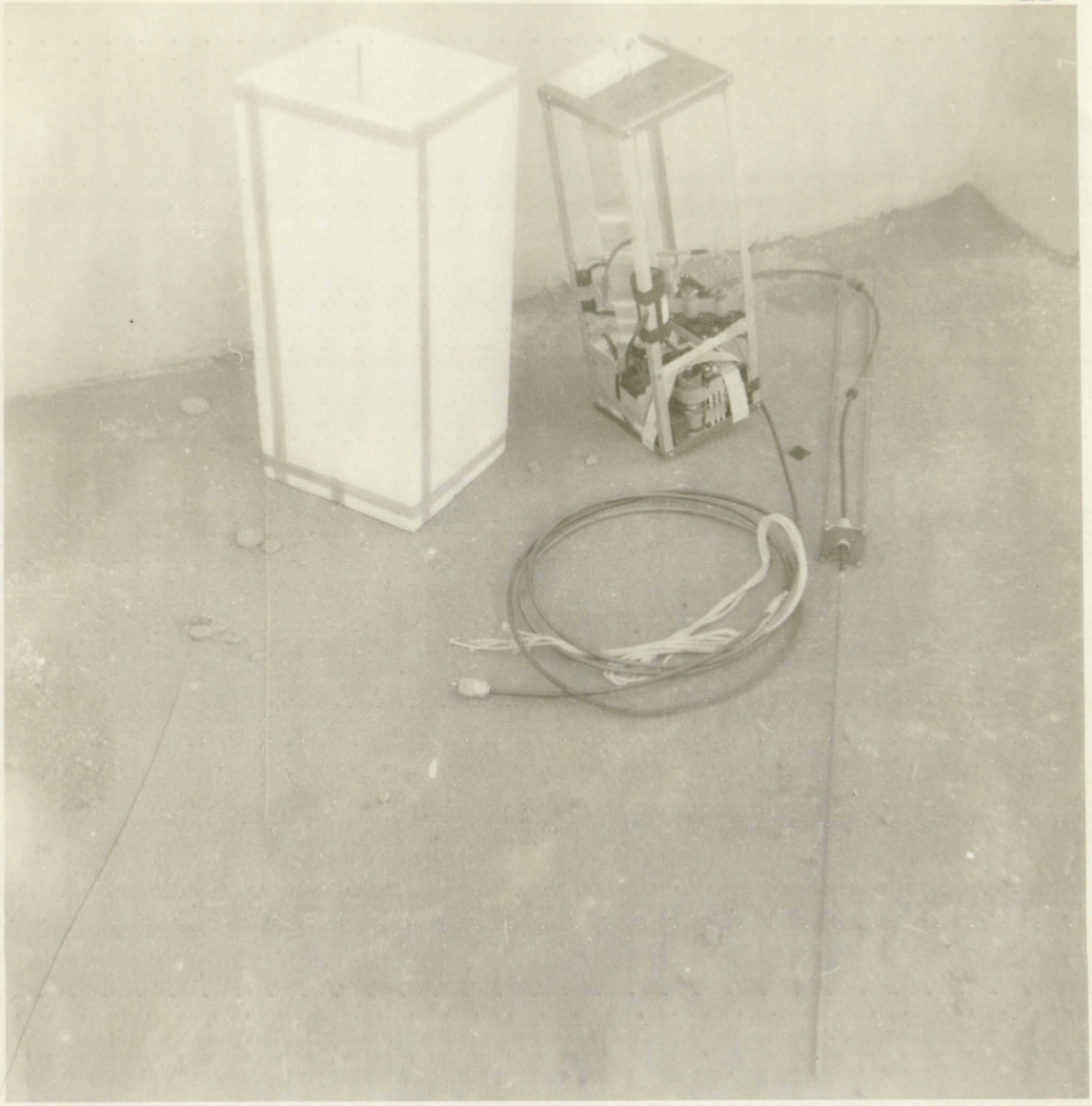

Figure 5. Photograph of gondola showing power supply and Geiger counter with Styrofoam case.

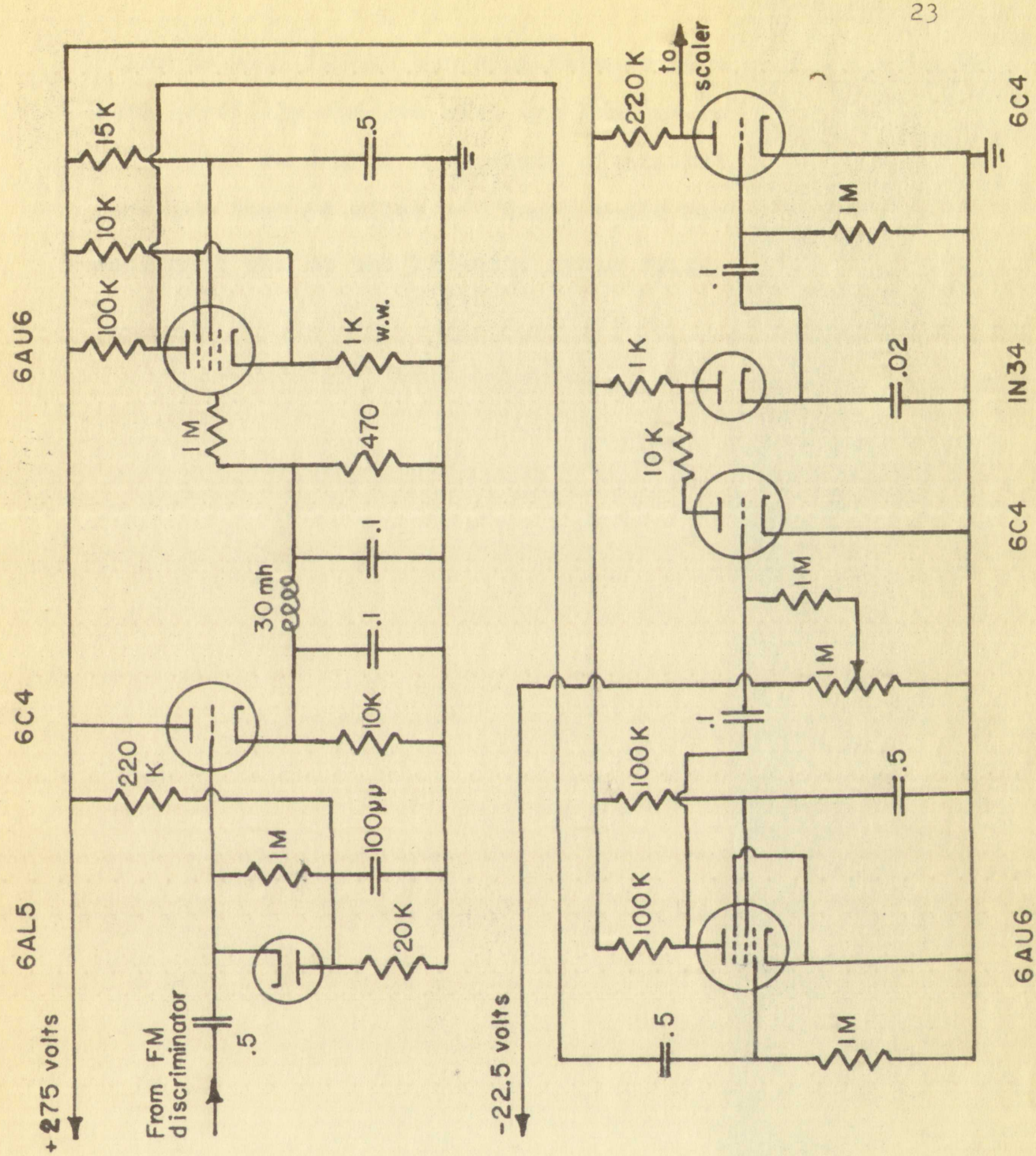

Figure 6. Schematic diagram of the saturation amplifier and integrating circuit.

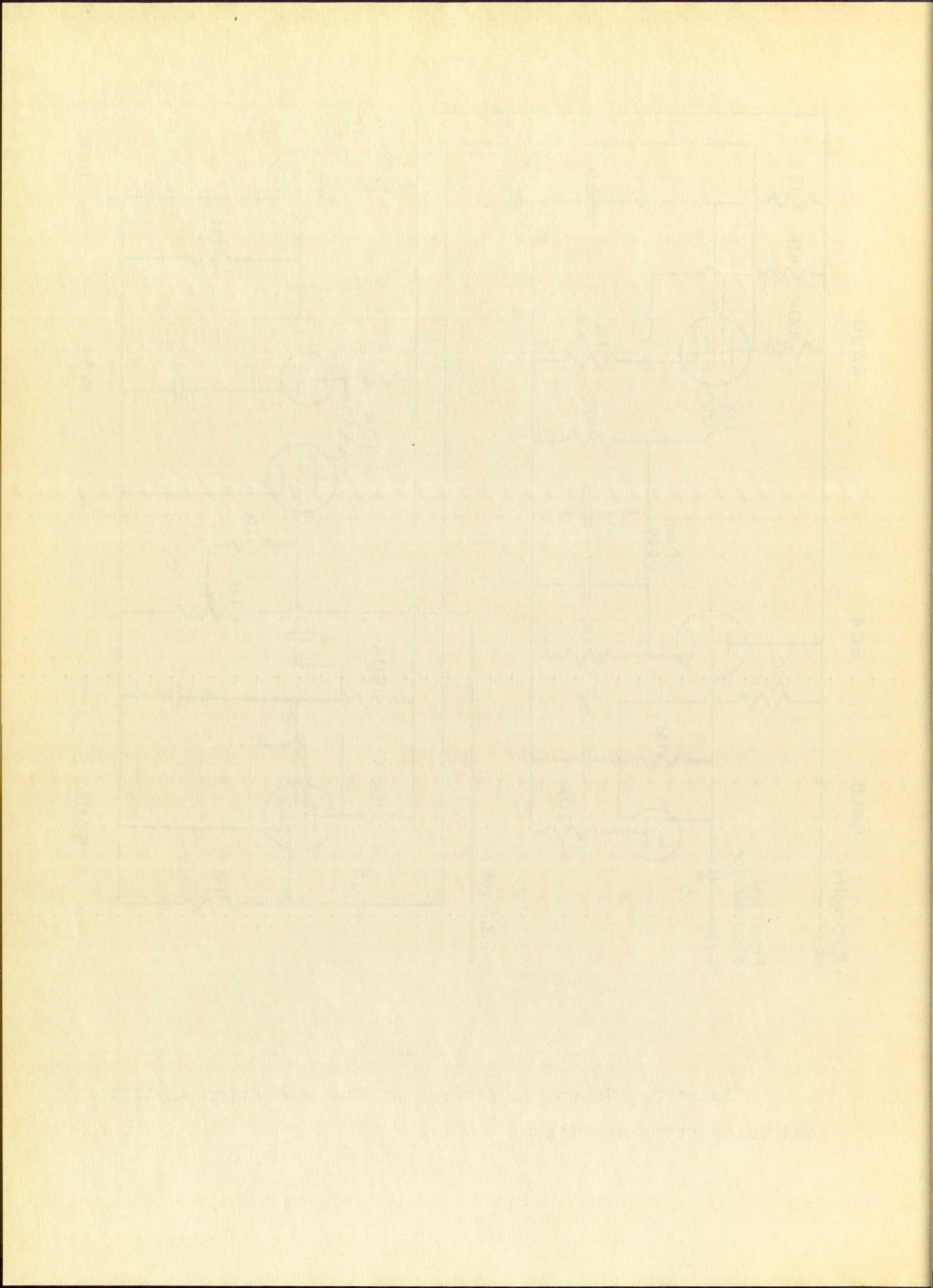

Prior to each flight the wind data at high altitudes were carefully checked with the Weather Bureau so that no flights were made when winds of excessive speeds (greater than 60 miles per hour) would have carried the equipment out of the 125-mile radio range.

CHAPTER IV

RESULTS

A. History of Flights

A total of seven flights was made during the month of April, 1954, all of which were launched from the Physics Building at the University of New Mexico in Albuquerque. Of these flights, one furnished accurate data for most of the flight, while two others gave accurate data for only short portions of the time in the air. No information of consequence was obtained from the other four flights. A summary of all the flights is shown in Table II.

On flights 1, 3, 4, and 5, the counters went into continuous discharge before the position of maximum intensity was reached. It is believed that due to insufficient thermal insulation of the counter at the extreme temperatures (-60°C.) encountered, condensation of the quenching gas, ether, took place and lowered the potential of the Geiger threshold. For a sufficient drop in threshold, the regulated 1200 volt power supply would send the tube into continuous discharge and thus permanently damage it. The difficulties were believed to be overcome by thermally insulating the Geiger counter in a snugly fitting Styrofoam jacket.

On flight 2 the counter operated properly for the entire flight. However, due to excessive wind velocities aloft, the swinging of the antenna and the gondola caused

TABLE II

SUMMARY OF FLIGHTS

Number of Flight	Date 1954	Time Launched MST A.M.	Remarks
1.	April 3	11:30	Counter went into continuous discharge at 30,000 feet.
2.	April 6	11:30	Antenna swinging caused signal fading. Counter satisfactory.
3.	April 13	11:30	Counter went into continuous discharge at 60,000 feet.
4.	April 14	11:30	Same as flight 1.
5.	April 17	11:30	Same as flight 1.
6.	April 20	11:30	No major difficulties were encountered.
7.	April 23	11:00	Same as flight 1.

the signal received at the ground to fade in and out due to changes in orientation of the balloon borne antenna relative to the antenna on the ground. By increasing the length of the antenna cable, and by lengthening the gondola-balloon distance from 20 feet to 50 feet, the swinging and consequent fading were reduced.

The counter tube in flight 7 was recovered from flight 2, and was evidently near the end of its useful life at the time of launching. After several minutes in the air, the tube went into continuous discharge.

Flight 6 was the only successful flight. During the three hours of recording, the signal received at the ground station was clear and was interrupted only for short periods by noise.

B. Interpretation of Data

In Figures 7, 8, and 9, plots of the counting rate vs. time are shown for the three fairly successful flights. The general shape of the curve, discussed in section A of Chapter 1, is apparent from Figures 7 and 9. The maximum counting rate occurred after about one hour in the air, and the minimum, when one balloon broke, after approximately one and one-half hours of flight. From here on the balloon descended and the curve passes through a maximum again. The one reliable curve, Figure 7, gives a counting rate of 93.1 ± 1.2 sec^{-1} for the ascent maximum at about 60,000 feet, and 93.2 ± 1.2 sec^{-1} for the descent maximum. If the dead

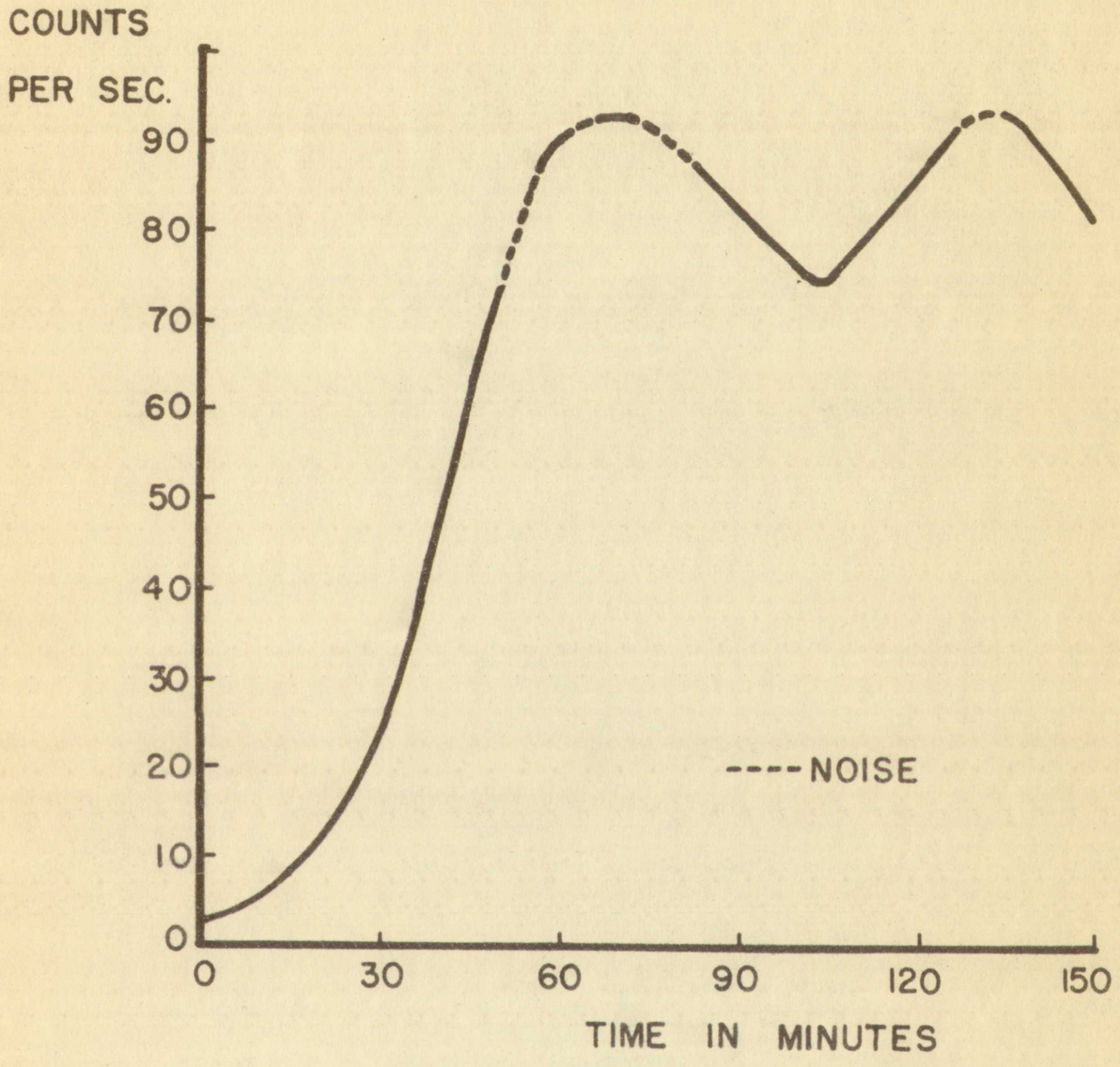

Figure 7. Counting rate, uncorrected for dead time, for flight 6.

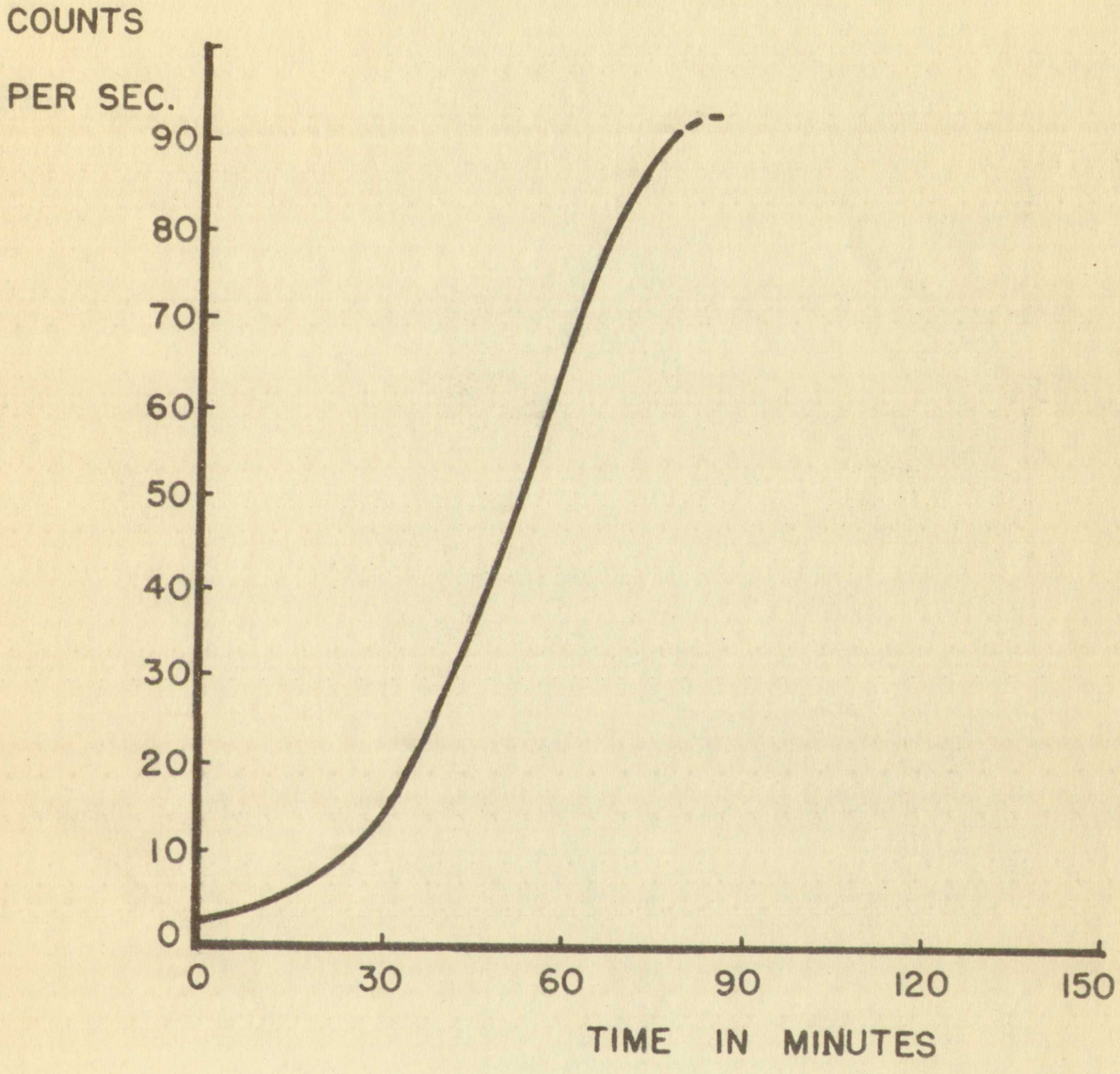

Figure 8. Counting rate, uncorrected for dead time, for flight 3.

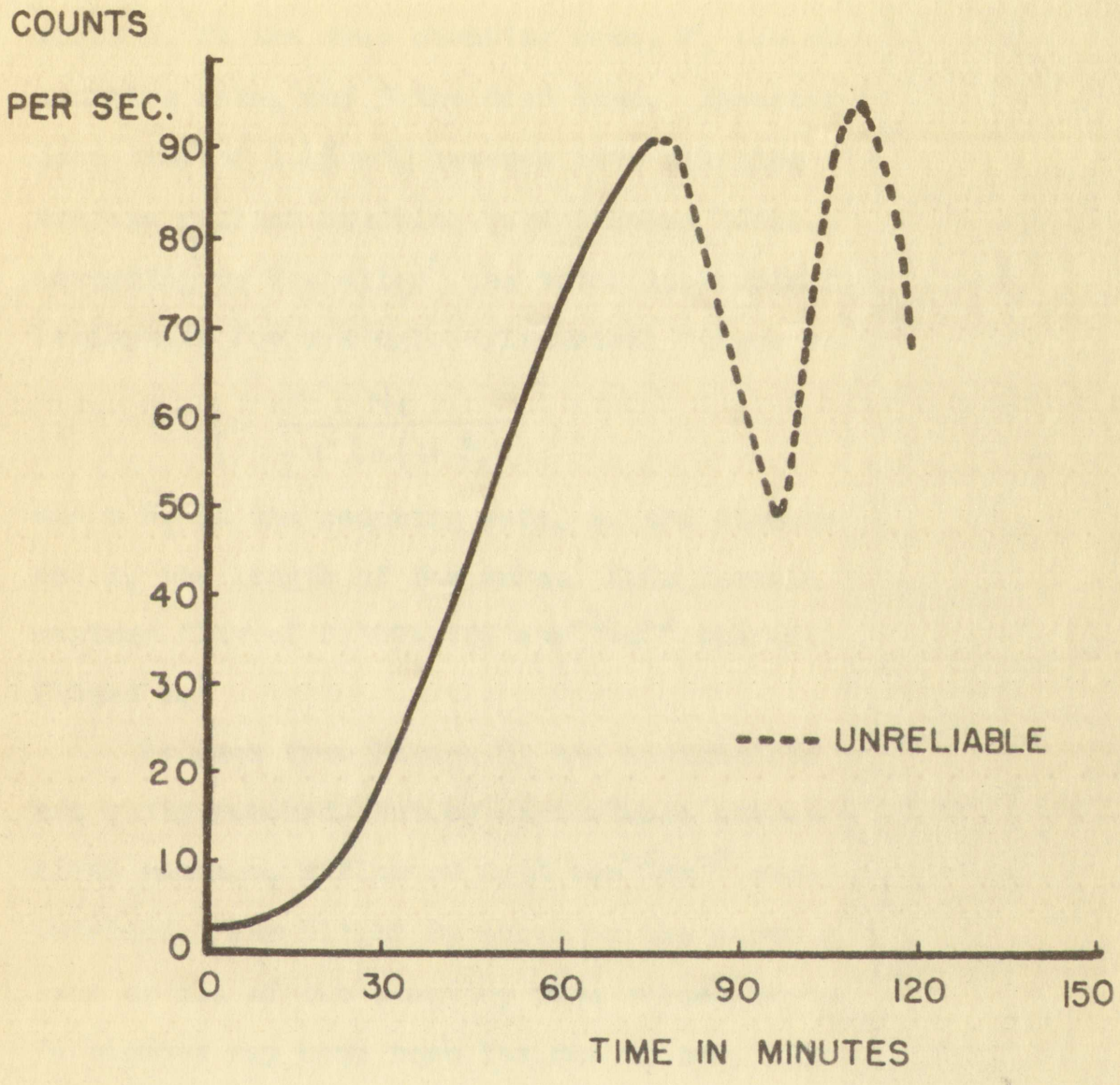

Figure 9. Counting rate, uncorrected for dead time, for flight 2.

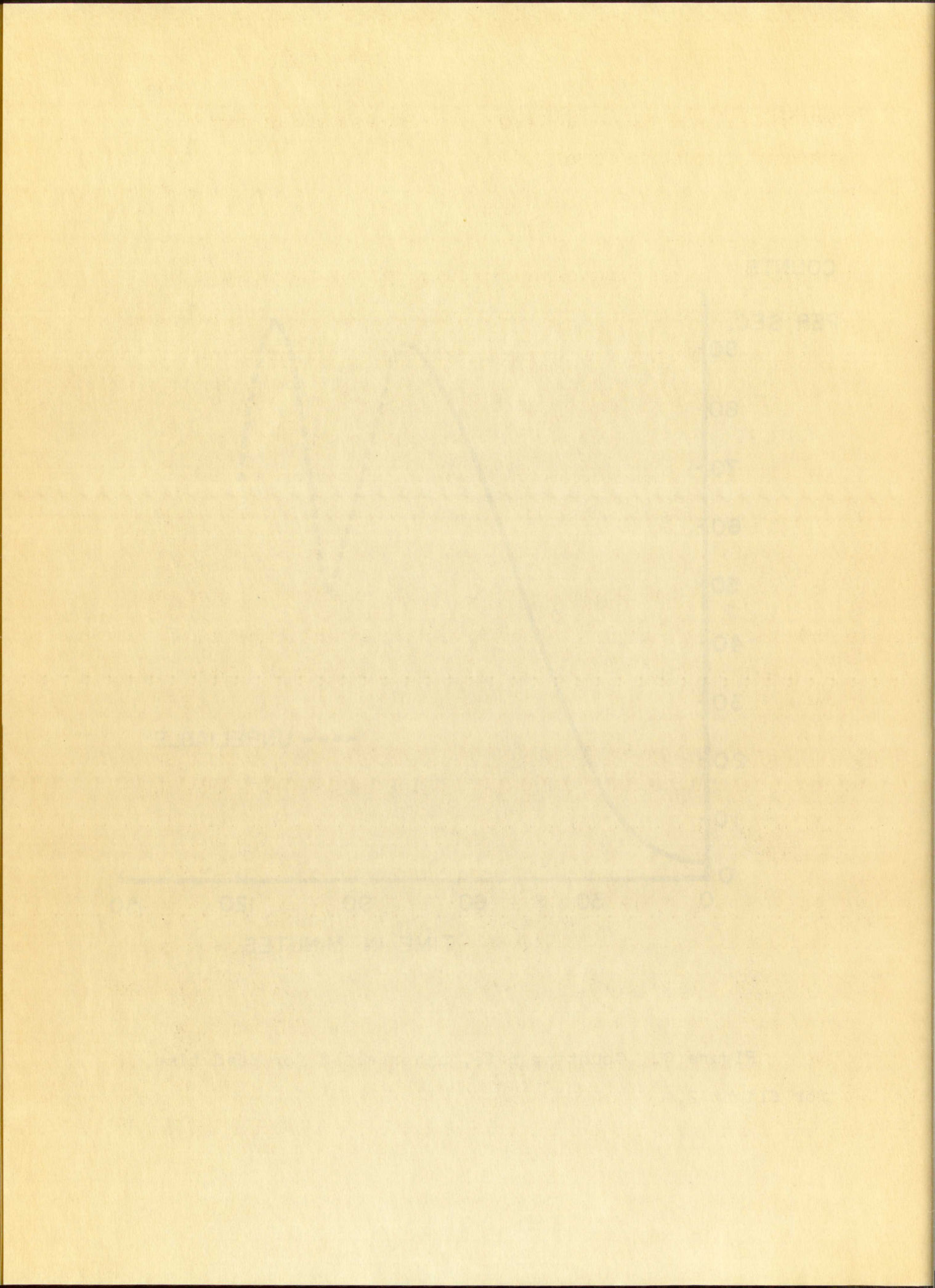

time of the counter is taken into consideration the true counting rate is given by:[7]

$$N_t = \frac{N_s}{1 - N_s \tau} , \qquad (16)$$

where N_t is the true counting rate, N_s the observed counting rate, and τ the dead time. Inserting the measured dead time of 1.45 milliseconds into equation (16), the average maximum counting rate becomes 108 ± 1.4 sec^{-1}. According to Van Allen[8] the total isotropic flux over one hemisphere for a single cylindrical Geiger counter is:

$$j = \frac{N_t}{\frac{1}{2}\pi^2 l a \left(1 + \frac{a}{2l}\right)} , \qquad (17)$$

where N_t is the counting rate, a, the diameter of the tube, and l, the length of the tube. This formula gives a maximum flux of $0.369 \pm .005$ $sec^{-1} cm^{-2}$ $steradian^{-1}$ for flight 6.

As seen from Figure 8, the maximum for flight 3 was not quite reached, but by approximate extrapolation to the first maximum, a flux of 0.38 $sec^{-1} cm^{-2}$ $steradian^{-1}$ is obtained. For flight 2, shown by the curve in Figure 9, some or all of the counting rate values beyond the first 75 minutes may have been low due to some signal loss from the swinging antenna. However, by averaging the intensities at the first and second maxima, an average maximum flux of 0.37 $sec^{-1} cm^{-2}$ $steradian^{-1}$ is obtained.

CHAPTER V

CONCLUSIONS

The effect of atmospheric depth on counting rate was observed by sending aloft balloon-borne cosmic ray counters. A maximum counting rate of 108 ± 1.4 sec^{-1} and a maximum flux of $0.369 \pm .005$ $sec^{-1}cm^{-2}$ $steradian^{-1}$ were obtained at an approximate atmospheric depth of 74 $gmcm^{-2}$. The ascent and descent maxima were well within experimental error of each other.

In 1947 Van Allen[8] obtained with a single Geiger counter a primary radiation flux above the atmosphere of 0.12 $sec^{-1}cm^{-2}$ $steradian^{-1}$ at a geomagnetic latitude of 41° N. He obtained a peak counting rate of 49 sec^{-1} at an altitude of 65,000 feet with a counter 6" long and 0.95" in diameter. That rate corresponds to a maximum flux of .257 $sec^{-1}cm^{-2}$ $steradian^{-1}$ which is naturally smaller than the value found in this experiment since Van Allen's data were obtained 4° closer to the geomagnetic equator.

Winckler[9] has performed experiments similar to the one described in this thesis. With a single Geiger counter 1" in diameter and 4 7/8" long, he obtained a maximum counting rate of 48 sec^{-1} at a geomagnetic latitude of 40° N. and 78 sec^{-1} at 53°N. These figures, after having been interpolated to a latitude of 45°N, indicate a maximum flux of about 0.35 $sec^{-1}cm^{-2}$ $steradian^{-1}$ which corresponds

favorably with the value reported here.

In conclusion, I wish to acknowledge the invaluable advice and help received from Dr. R. R. Brown during the course of these experiments.

BIBLIOGRAPHY

BIBLIOGRAPHY

1. Van Allen, J. A. "The Cosmic Ray Intensity above the Atmosphere near the Geomagnetic Pole," Department of Physics, State University of Iowa (1953).

2. Kane, E. O., Shanley, T.B.J., and Wheeler, J. A. Reviews of Modern Physics, 21, 51 (1949).

3. Dwight, K. Physical Review, 78, 40 (1950).

4. Fermi, E. "Nuclear Physics," The University of Chicago Press (1950).

5. Chapman, S. Nature, 140, 423 (1937).

6. Wilson, J. G. "Progress in Cosmic Ray Physics" New York: Inter-science Publishers inc. (1952).

7. Wilkinson, D. H. "Ionization Chambers and Counters" Cambridge: The University Press (1950).

8. Van Allen, J. A., and Tatel, H. E. Physical Review, 73, 245 (1948).

9. Winckler, J. R., and Baskin, R. Unpublished report on "A Study of Cosmic Ray Time Variations with a Single Geiger Counter Radiosonde" (1953).

Date Due			
MAR 2 4 1958			
MAR 8 1958			
MAR 8 RECD			
JUN 4 - 1960			
MAY 2 7 RECD			
APR 4 1961			
APR 4 - RECD			
MAY 27 1961			
MAY 19 RECD			


DIETER
BINDS
BETTER
DENVER COLO